Quantifying the missing link between forest albedo and productivity in the boreal zone

Aarne Hovi[1], Jingjing Liang[2], Lauri Korhonen[3], Hideki Kobayashi[4], Miina Rautiainen[1,5]

[1]Department of Built Environment, School of Engineering, Aalto University, P.O.Box 15800, 00076 AALTO, Finland

[2]School of Natural Resources, West Virginia University, P.O.Box 6125, Morgantown, WV 26505, USA

[3]School of Forest Sciences, University of Eastern Finland, P.O.Box 111, 80101 Joensuu, Finland

[4]Department of Environmental Geochemical Cycle Research, Japan Agency for Marine-Earth Science and Technology, 3173-25, Showa-machi, Kanazawa-ku, Yokohama, 236-0001, Japan

[5]Department of Radio Science and Engineering, School of Electrical Engineering, Aalto University, P.O. Box 13 000, 00076 AALTO, Finland

Correspondence to: Aarne Hovi (aarne.hovi@aalto.fi)

15 **Abstract.** Albedo and fraction of absorbed photosynthetically active radiation (FAPAR) determine the shortwave radiation
16 balance and productivity of forests. Currently, the physical link between forest albedo and productivity is poorly understood,
17 yet it is crucial for designing optimal forest management strategies for mitigating climate change. We investigated the
18 relationships between boreal forest structure, albedo and FAPAR using radiative transfer model FRT and extensive forest
19 inventory data sets ranging from southern boreal forests to the northern tree line in Finland and Alaska (N = 1086 plots). The
20 forests in the study areas vary widely in structure, species composition, and human interference, from intensively managed in
21 Finland to natural growth in Alaska. We show that FAPAR of tree canopies (FAPAR$_{CAN}$) and albedo are tightly linked in
22 boreal coniferous forests, but the relationship is weaker if the forest has broadleaved admixture, or if canopies have low leaf
23 area and the composition of forest floor varies. Furthermore, the functional shape of the relationship between albedo and
24 FAPAR$_{CAN}$ depends on solar angle. We also show that forest floor can contribute to over 50% of albedo or total ecosystem
25 FAPAR. Based on our simulations, forest albedos vary notably across the biome. Because of larger proportion of
26 broadleaved trees, the forests in Alaska have higher albedo (0.141–0.184) than those in Finland (0.136–0.171) even though
27 the albedo of pure coniferous forests is lower in Alaska. Our results reveal that variation in solar angle will need to be
28 accounted for when evaluating climate effects of forest management in different latitudes. Furthermore, increasing the
29 proportion of broadleaved trees in coniferous forests is the most important means of maximizing albedo without
30 compromising productivity: based on our findings the potential of controlling forest density (i.e., basal area) to increase
31 albedo may be limited compared to the effect of favoring broadleaved species.

33 Keywords: FAPAR, conifer, broadleaved, radiative transfer, basal area, leaf area index, AGB, thinning

1   Introduction

Forest management practices, such as thinning and logging, alter the spatial, structural, and species composition of forests. Through an altered albedo and productivity, these management practices may cause profound impacts on climate. Because forest structure and species composition influence albedo, managing forests to increase albedo is a potential means of maximizing the climate cooling effects of forests (Bright et al., 2014; Alkama & Cescatti, 2016; Naudts et al., 2016). However, if forest management practices are altered in order to maximize albedo, productivity may be compromised, which would result in reduced carbon uptake as well as reduced timber production and corresponding economic losses. There is an urgent need to understand how forest management practices change forest albedo, and how forest albedo and productivity are interconnected.

Being the world's largest land-based biome, the boreal forest zone consists of vast forest areas under various human interference levels, from natural growth to intense silvicultural management. The biome plays an important role in controlling the global carbon and energy balances. It is estimated that the boreal forests comprise 32% of the total carbon in the world's forests, and account for a significant portion of the carbon uptake (Pan et al., 2011). In addition, the albedo of boreal forests varies considerably by forest structure, phenology, and snow cover (e.g., Ni & Woodcock, 2000; Kuusinen et al., 2012; Bright et al., 2013; Kuusinen et al., 2016).

Previous studies based on local in situ measurements, or remote sensing data for local to regional study areas have shown that boreal forest albedo is influenced by tree species, with broadleaved species rendering higher albedos than coniferous (Lukeš et al., 2013a, Kuusinen et al., 2014). Albedo of open areas or that of the forest floor is usually higher than in the canopy areas (Bright et al., 2014, Kuusinen et al., 2014), except for burned sites (Amiro et al., 2006). A declining trend in albedo with forest height or age has been observed for coniferous forests (Amiro et al., 2006; Kirschbaum et al., 2011; Bright et al., 2013; Kuusinen et al., 2016) and may be at least partly explained by the increasing leaf area index (LAI) and thus reduced contribution of the forest floor on albedo as the forests mature. Similarly, a declining trend in albedo with canopy density has been observed (Lukeš et al., 2013a).

Gross primary productivity of vegetation can be approximated by FAPAR, i.e. the fraction of PAR radiation (400–700 nm) absorbed by the vegetation canopy (Gobron & Verstraete, 2009), because photosynthesis is ultimately driven by the available solar energy. FAPAR is useful in monitoring and comparing productivity both spatially and temporally, especially in the absence of accurate growth and yield models. The main determinants of forest canopy FAPAR are leaf area index (LAI) and the directionality of incoming solar radiation (Majasalmi et al., 2014), because they determine the fraction of PAR radiation interceptable by the canopy. Similarly to albedo, boreal forest FAPAR may differ by tree species (Roujean et al.,

66 1999; Steinberg et al., 2006; Chasmer et al., 2008; Serbin et al., 2013; Majasalmi et al., 2015) and stand age (Serbin et al.,

67 2013), as both species and age are likely to influence the LAI of the canopy.

68

69 Estimation methods set limits for the information that can be obtained on the spatial and temporal variation of albedo and

70 FAPAR. In situ measurements are accurate and can be directly linked with field measured forest structure. On the other

71 hand, they are extremely tedious and cannot cover large variations in forest structure. Satellite data provide ample coverage

72 of varying forest structures and wide spatial extent but may compromise spatial resolution and detail in the characterization

73 of forest structure. In addition, neither local albedo measurements nor satellite-based albedo products can explain the

74 causality between small-scale environmental management scenarios and changes in albedo or FAPAR. Radiative transfer

75 models offer a solution to these problems: forest radiative transfer models are a powerful tool for linking quantitative

76 changes in vegetation structure to albedo or FAPAR for large geographical regions. The models are parameterized using

77 mathematical descriptions of canopy structure (e.g., LAI, tree height, crown dimensions, stand density), optical properties of

78 foliage and forest floor, and spectral and angular properties of incoming radiation. Using these models, the albedo and

79 FAPAR of a forest can be calculated from readily measurable variables such as forest structure and leaf optical properties.

80

81 To date, studies on forest structure and albedo have mainly focused on specific geographical areas (e.g. Finland, Norway, but

82 see Kuusinen et al. (2013) for comparison between Finland and Canada). Comparison of the relationships between forest

83 structure, albedo and FAPAR has not been performed across the biome, i.e. including both European and North American

84 boreal forests which have very different natural structures and forest management scenarios. Due to the large north-south

85 gradient and consequent structural diversity of forests in the boreal zone, the impact of forest management on albedo cannot

86 be expected to be the same. In addition, while the relations of albedo and FAPAR to forest structure have been locally

87 studied in boreal forests, the explicit link between FAPAR and albedo has not been shown.

88

89 Here we report results from quantifying the links between boreal forest structure, albedo and FAPAR ranging from southern

90 boreal forests to the northern tree line using detailed, large forest inventory data sets from Finland and Alaska (N = 1086

91 plots). The forests in the study areas vary widely in structure, species composition, and human interference, from intensively

92 managed (regularly thinned) forests in Finland to natural growth in Alaska. Using a radiative transfer modeling approach, we

93 quantify the effects of forest structure and species composition on albedo and FAPAR in order to answer how forest

94 management practices can be optimized for climate change mitigation. The significant benefit of the modeling approach is

95 that it enables to study structurally varying forests over large geographical areas, without compromising detail in the forest

96 structure representation or in the spatial resolution. Our study is therefore the first intercontinental study connecting albedo

97 and productivity of boreal forests, using accurate ground reference data.

2 Materials and methods

2.1 Study areas and field plots

This study is based on 1086 field plots located in Alaska, USA, and in Finland, between Northern latitudes of 60° and 68°. At these latitudes, solar zenith angle (SZA) at solar noon at midsummer ranges from 37° to 45°, and the annual average from 69° to 72°.

The field plots in Alaska (N = 584) were permanent sample plots established as part of Co-operative Alaska Forest Inventory that aims at long-term monitoring of forest conditions and dynamics (Malone et al., 2009). The plots were scattered in interior and southcentral Alaska across a region of about $300\,000\ km^2$, from Fairbanks in the north to the Kenai Peninsula in the south (Fig. 1, for more details see Liang et al. (2015)). Some of the plots were measured more than once. We used only the most recent measurement of each plot. The plots in Finland (N = 502) were temporary or permanent sample plots. They were located at four separate sites: Hyytiälä (Majasalmi et al., 2015), Koli, Sodankylä, and Suonenjoki (Korhonen, 2011) ranging from southern to northern Finland (Fig. 1). Species-level attributes, including the number of stems per hectare, basal area, mean diameter at breast height, tree height, and length of living crown, were available for the plots. Basal area, the total cross-sectional area of stemwood ($m^2\ ha^{-1}$) at breast height (i.e. at 1.3 m or 1.37 m), is a common measure of stand density in forest inventories and, combined with information on tree height, used as an indicator of need for silvicultural thinning operations.

Tree species in the Alaskan data were coniferous black spruce (*Picea mariana* (Mill.) B. S. P.) and white spruce (*Picea glauca* (Moench) Voss), and broadleaved quaking aspen (*Populus tremuloides* Michx.), black cottonwood or balsam poplar (*Populus trichocarpa* Torr. & Gray, *P. balsamifera* L.), Alaskan birch (*Betula neoalaskana* Sarg.), and Kenai birch (*Betula kenaica* W.H. Evans). Tree species in the Finnish data were coniferous Scots pine (*Pinus sylvestris* L.) and Norway spruce (*Picea abies* (L.) H. Karst), and broadleaved species comprising mainly of silver and downy birch (*Betula pendula* Roth, *B. pubescens* Ehrh.). The birches accounted for 89% of the basal area of the broadleaved species in Finland. The forest variables in the study plots are shown in Table 1, for all plots and separately for plots dominated by one species. The Alaskan and Finnish forests differed in structure. The forests in Alaska were on average denser in terms of basal area (Fig. 2), and contained larger proportion of broadleaved species than the Finnish forests (Table 1). Managed forests in Finland, which our plots mainly represent, are normally thinned 1–3 times during the rotation period so that coniferous species are favored. In our plots from Alaska, on the other hand, no thinnings were applied.

The plots in Finland were classified into six site fertility classes in the field, according to a local site type classification system (Cajander, 1949). We re-classified the original number of six fertility classes into three: "xeric", "mesic", and "herb-rich". The cover of grasses is highest in the herb-rich, and decreases towards the xeric type. The cover of lichens, on the

131 other hand, increases towards the xeric type (Hotanen et al., 2013). In the Alaskan plots no site fertility estimate was

132 available but the cover of each species in the forest floor had been estimated. We labeled the plots as lichen- or grass

133 dominated if either the cover of lichens or the total cover of herbs, grasses, rush, sedges, and fern was over 50%. The

134 remaining plots were dominated by shrubs and mosses or were a mixture of all species groups. Hereafter we refer to these

135 forest floor types as "grass", "shrub/moss", and "lichen". Forest floor types did not differ notably between forests dominated

136 by different tree species, except for Scots pine forests in Finland, which were often found in the xeric type and were almost

137 nonexistent in the herb-rich type (Table 2).

2.2   Albedo and FAPAR simulations

2.2.1   Simulation model

140 We simulated albedo and FAPAR using a radiative transfer model called Forest Reflectance and Transmittance model FRT

141 (Kuusk & Nilson, 2000, version modified by Mõttus et al., 2007). FRT is a hybrid type model that combines geometric-

142 optical and radiative transfer based sub-models for modeling the first- and higher-order scattering components, respectively.

143 The model has been intercompared and validated within RAdiative transfer Model Intercomparison exercise (RAMI) several

144 times (Widlowski et al., 2007). The advantage of FRT is that it can be parameterized using standard forest inventory data,

145 utilizing the allometric relations of forest variables to foliage biomass and crown dimensions. This was important because

146 field measurements of biophysical variables (e.g., LAI) are not commonly available, as in our study plots.

147

148 FRT simulates stand-level bidirectional reflectance and transmittance factors (BRF, BTF) of a forest at specified

149 wavelengths. A 12×12 Gauss-Legendre cubature was used to integrate the simulated BRF and BTF values over the upper

150 and lower hemispheres, respectively. The resulting upward (top of canopy) and downward (below canopy) fluxes were then

151 used to calculate the shortwave broadband albedo and FAPAR. The simulations were carried out at 5 nm resolution, and the

152 albedo simulations covered a spectral region of 400−2100 nm which corresponds to the region from which input data was

153 available (see Section 2.2.2). The wavelengths below 400 nm account for 8%, and wavelengths over 2100 nm account for

154 2% of the solar irradiance on top of the atmosphere (Thuillier et al., 2003). The simulations were performed assuming direct

155 illumination only, i.e. in black sky conditions. Black sky albedo is, compared to actual (blue sky) albedo, less dependent on

156 assumptions of atmospheric scattering properties. It is commonly used as input in climate modeling (Schaaf et al., 2009). We

157 repeated the simulations at five SZAs typical for the study areas. These were 40°, 50°, 60°, 70°, and 80°. We use terms

158 "small SZA" and "large SZA" in the text hereafter, to refer to SZAs of 40°–50° and 70°–80°, respectively. It should be noted

159 that small SZA refers to the situation where the sun is at its highest position.

160

161 The shortwave black sky albedo, hereafter referred to as "albedo", was obtained as a weighted sum of the spectral albedos,

162 i.e. upward fluxes ($flux_l$ -), on top of canopy:

163

$$albedo = \sum_{l=400}^{2100} w_l \times flux_l{\text -} ,$$ (1)

165

166 The canopy and total FAPAR (FAPAR$_{CAN}$, FAPAR$_{TOT}$) were obtained as weighted sums of canopy absorption (a_l^C) and

167 total absorption (a_l^T) over the PAR region:

168

$$FAPAR_{CAN} = \sum_{l=400}^{700} w_l \times a_l^C ,$$ (2)

170

$$FAPAR_{TOT} = \sum_{l=400}^{700} w_l \times a_l^T ,$$ (3)

172

173

174 The weights (w_λ) were obtained from the standard reference solar irradiance spectrum on top of the atmosphere (Thuillier et

175 al., 2003). To obtain the weights, the solar irradiance values (W m^{-2}) were scaled by dividing them with the total solar

176 irradiance within the spectral region used (i.e., 400–2100 or 400–700 nm). The weights were thus unitless and summed up to

177 unity. FAPAR$_{TOT}$ and FAPAR$_{CAN}$ were separated because the former is a measure of total ecosystem productivity whereas

178 the latter is more closely linked with timber production. Our FAPAR$_{TOT}$ does not separate green biomass from litter and the

179 values therefore represent an upper limit of productivity.

180

181 The canopy and total absorptions needed for FAPAR determination were obtained using upward flux on top of canopy (

182 $flux_l{\text -}$), downward flux below canopy ($flux_l{\text{ }}^-$), and the reflectance factor of the forest floor (r_G) as follows:

183

184 $$a_l^C = 1{\text -} flux_l{\text -} {\text -} flux_l{\text{ }}^- + r_l^G \times flux_l{\text{ }}^- ,$$ (4)

185

186 $$a_l^T = 1{\text -} flux_l{\text -} ,$$ (5)

187

188 Both $flux_l{\text -}$ and $flux_l{\text{ }}^-$, and therefore also a_l^C and a_l^T , are unitless fractions of the total incoming solar irradiance.

189

2.2.2 Model parameters

Tree crowns are represented in the FRT model by geometric primitives (cylinders or ellipsoids). The foliage within a crown is assumed to be homogeneously distributed. The area volume density (area per unit crown volume) of the foliage depends on the crown dimensions and on the foliage area per tree. Several tree classes can be defined to represent different tree species or size classes. We used one class for each tree species. Because the maximum number of species was seven in the Alaskan data, there was a maximum of seven tree classes per plot. We assumed ellipsoid crown shape which estimates the crown volume accurately (Rautiainen et al., 2008). Crown length was obtained from field measurements, and the crown radius was modeled using species-specific allometric equations that require stem diameter as independent variable (Jakobsons, 1970; Bragg, 2001). Leaf dry biomass was estimated with species-specific biomass equations (Repola, 2008; Repola, 2009; Yarie et al., 2007) and converted into hemisurface i.e. half of total leaf area, using leaf mass per area (LMA) values from literature (Table 3). A slightly regular spatial distribution pattern of trees was assumed, i.e. a value of 1.2 for the tree distribution parameter (a value of 1 indicates Poisson distribution, Nilson, 1999). Other structural parameters needed in FRT simulations are presented in Table 3.

Optical properties i.e. reflectance and transmittance of the leaves and needles were obtained from laboratory spectrometer measurements. The data for Finnish species were from Hyytiälä, Finland (Lukeš et al., 2013b). Spectra of birch were used for all broadleaved species. The data for Alaskan species were from Superior National Forest, Minnesota, USA (Hall et al., 1996). Data for all species could not be found separately, and therefore spectra of black spruce were used for both black and white spruce, spectra of paper birch (*Betula papyrifera* Marsh.) were used for both birch species, and spectra of quaking aspen were used for both quaking aspen and for the black cottonwood/balsam poplar group. Reflectance spectra of black and white spruce needles have been found to be similar at least in the visible and near-infrared wavelengths (Richardson et al., 2003). In our data, the spectra of coniferous species did not differ notably from each other (Fig. 3a). The same applied to broadleaved species. Bark spectra for spruces and *Populus* sp. in Alaska were obtained from Hall et al. (1996), and for Scots pine and Norway spruce in Finland from Lang et al. (2002) (Fig. 3b). Spectra of birch from Lang et al. (2002) were used for birches in Alaska and for broadleaved species in Finland.

We used the annual shoot as a basic scattering element for conifers, similarly as in Lukeš et al. (2013a). This accounts for the multiple scattering within shoot which results in the shoot albedo being lower than needle albedo. Shoot reflectance and transmittance spectra were obtained by upscaling the needle single scattering albedo to shoot albedo (Rautiainen et al., 2012), assuming that the reflectance to transmittance ratio of a shoot is equal to that of a needle. Bi-Lambertian scattering properties of the scattering elements (leaves or shoots) were assumed.

222 Optical properties of the forest floor, i.e. reflectance factors at nadir view were obtained from field spectrometer
223 measurements. The data were collected from Poker Flat Research Range Black Spruce Forest, Alaska (measurements
224 described in Yang et al. (2014)), and from Hyytiälä, Finland (using similar methodology as in Rautiainen et al. (2011)).
225 Separate spectra for each forest floor type was used (Fig. 3c), because characteristics of the forest floor may influence the
226 forest reflectance and therefore also albedo (Rautiainen et al., 2007).

2.3 Data analyses

2.3.1 Albedo, FAPAR, and forest structure

229 We analyzed albedo and FAPAR ($FAPAR_{CAN}$, $FAPAR_{TOT}$) against each other, and against the forest variables. The analyses
230 were performed separately for Alaskan and Finnish data, and repeated for all simulated SZAs. Because of the strong
231 emphasis on forest management, main focus of the analysis was on tree species and tree height which are usually measured
232 as part of forest inventories. In addition, we analyzed albedo and FAPAR against effective leaf area index (LAI_{eff}) and above
233 ground biomass (AGB). LAI_{eff} is calculated by FRT, and corresponds to the LAI of a horizontally homogeneous, optically
234 turbid canopy that has exactly the same transmittance (gap probability) as the canopy under examination. AGB was
235 calculated with individual-tree allometric equations (Repola, 2008; Repola, 2009; Yarie et al., 2007), similarly as the foliage
236 biomass.

238 In the next phase, all simulations were repeated assuming black soil (i.e., a totally absorbing background), in order to better
239 explain the dependencies of albedo on tree height and SZA as well as to explain the differences of albedo between Alaskan
240 and Finnish forests. The albedo obtained in black soil simulation represents the plain canopy albedo without the contribution
241 of forest floor vegetation. We refer to this as "canopy contribution". Correspondingly, the contribution of forest floor can be
242 calculated by subtracting the canopy contribution from the albedo obtained when assuming a vegetated forest floor. We refer
243 to this as "forest floor contribution". Canopy and forest floor contributions can be expressed as absolute values or relative
244 values which sum up to 100%. For comparison with the results regarding albedo, the forest floor contribution to total
245 ecosystem FAPAR was also calculated, by subtracting $FAPAR_{CAN}$ from $FAPAR_{TOT}$.

247 We report the relationships of albedo and FAPAR against forest structure in Sect. 3.1. Results of these experiments are
248 needed for understanding the relations between albedo and FAPAR, which we report in Sect. 3.2.

2.3.2 Relative importance of density and tree species

250 To examine the relative importance of density and species composition, we analyzed albedo and $FAPAR_{CAN}$ against basal
251 area and the proportion of broadleaved trees. The analyses were performed separately for Alaska and Finland, and repeated
252 for all simulated SZAs. We excluded all plots with tree height less than 10 m from the analyses in order to evaluate the effect

253   of basal area independent of tree height. This was done based on the following reasoning. Basal area was correlated with tree

254   height when studying all plots (r = 0.61 (Alaska), r = 0.64 (Finland)). Preliminary analysis was performed by successively

255   removing plots with smallest trees and each time checking the correlation between height and basal area. The correlation was

256   reduced until a height threshold of 10 m (r = 0.40 (Alaska), r = 0.34 (Finland)) (cf. Fig. 2). Therefore, the 10 m threshold was

257   used to exclude the smallest trees from our analyses. Analysis of albedo and FAPAR against basal area in this restricted set

258   of plots gives an approximation of how thinnings would affect albedo and $FAPAR_{CAN}$ although in reality thinning a stand

259   affects not only the basal area but also the spatial pattern and size distribution of trees.

261   Mean and standard deviation (SD) of albedo and $FAPAR_{CAN}$ in conifer-dominated forests were calculated for ten equally

262   spaced classes with respect to basal area. The center of the lowest class corresponded to the 5th and that of the highest class

263   to the 95th percentile of basal area in the data. To examine the effect of broadleaved proportion, mean and SD of albedo and

264    $FAPAR_{CAN}$ were calculated for ten equally spaced classes with respect to proportion of broadleaved trees, i.e. the

265   broadleaved proportions ranging from 0–10% to 90–100%. The analysis was repeated for sparse (basal area percentiles from

266   0th to 30th) and dense forest (basal area percentiles from 70th to 100th). We hypothesized that the proportion of broadleaved

267   trees would have smaller effect on albedo in sparse than in dense forest, because the forest floor has more significant role in

268   the sparse canopies. Results regarding the analysis of basal area and proportion broadleaved trees are reported in Sect 3.3.

269   3   Results

270   3.1   Albedo, FAPAR, and forest structure

271   Mean albedo of forests in Alaska (0.141–0.184) was higher than in Finland (0.136–0.171). In general, the albedo of

272   broadleaved species was 42–130% higher than that of coniferous (Table 4). However, albedo varied greatly even among

273   coniferous species: in Alaska, the albedo of white spruce forests was 20–33% higher than that of black spruce, and in

274   Finland, the albedo of Scots pine forests was 22–31% higher than that of Norway spruce. Overall, the mean albedo of

275   coniferous species was 28–32% higher in Finland (0.131–0.161) than in Alaska (0.102–0.122). The mean albedos of

276   broadleaved species in Alaska did not differ significantly from each other at any SZA (p > 0.05 in ANOVA), and therefore

277   the broadleaved species were treated as one group hereafter. Increasing the SZA increased the albedos of all species (Table

278   4).

280   The forest canopies in Alaska absorbed more PAR radiation than in Finland: mean $FAPAR_{CAN}$ in Alaska was 0.71–0.92 and

281   in Finland 0.63–0.89. $FAPAR_{CAN}$ increased with increasing SZA (Table 4). At the smallest SZA (40°) $FAPAR_{CAN}$ was

282   highest for broadleaved species in Alaska, followed by Norway spruce in Finland, white spruce in Alaska, and broadleaved

283   in Finland. Scots pine in Finland and black spruce in Alaska had lowest $FAPAR_{CAN}$ among the species. Similarly as for

284   albedo, the mean $FAPAR_{CAN}$ of broadleaved species in Alaska did not differ significantly from each other at any SZA (p >

285 0.05 in ANOVA). Increasing the SZA increased $FAPAR_{CAN}$ of all species and also reduced the differences between species.

286 The relative increase was smaller for broadleaved than for coniferous species. Therefore, the order of species in $FAPAR_{CAN}$

287 was different at small and large SZAs (Table 4). $FAPAR_{TOT}$, an approximation of total ecosystem productivity, ranged from

288 0.93 to 0.98. $FAPAR_{TOT}$ of coniferous forests was higher than that of broadleaved but the differences were not large in

289 relative terms because $FAPAR_{TOT}$ was consistently high.

290

291 Albedo decreased with increasing tree height in coniferous forests (Fig. 4). The decrease was most rapid at small tree heights

292 and saturated after the height reached approximately 10 m. When SZA increased, the difference in albedo between short and

293 tall forests became smaller (compare Fig. 4a,b to Fig. 4c,d). The albedo of broadleaved forests was similar for all tree heights

294 at the smallest SZA (40°). At large SZAs, however, there was an initial rapid increase in albedo for broadleaved forests with

295 small trees (Fig. 4d), after which the albedo remained stable. AGB was correlated with tree height (r = 0.72–0.78) and the

296 albedo responded to AGB with a similar saturating trend as in the case of tree height (Fig. 4e,f).

297

298 $FAPAR_{CAN}$ initially increased with increasing tree height, but saturated at large tree heights (Fig. 5). The saturation was

299 reached earlier and the maximum level of $FAPAR_{CAN}$ was higher at large SZAs. Similar saturating trends and SZA

300 dependencies were observed also against AGB although there was less variation in the y direction (Fig. 5e,f). $FAPAR_{TOT}$

301 increased as function of tree height in coniferous forests, and was stable in broadleaved forests (Fig. 6). However, the

302 variation in $FAPAR_{TOT}$ with tree height was small (values ranging from 0.93 to 0.98).

303

304 The average contribution of forest floor to total forest albedo depended on tree species and ranged from 4% to 53% (Table

305 5). It was largest at small SZAs and for tree species that had low LAI_{eff} (see LAI_{eff} values in Table 1). Forest floor

306 contribution decreased as a function of tree height (Fig. 7). The relation was even tighter when the forest floor contribution

307 was analyzed against LAI_{eff} (not shown). This is logical because LAI_{eff} is more directly linked with canopy transmittance

308 than is tree height. Increasing the SZA increased the canopy contribution in all plots. In general, the net effect was an

309 increase of albedo as a function of SZA. Only a few sparse canopies (low LAI_{eff}) were an exception. In these plots, an

310 increase in SZA reduced the forest floor contribution more than it increased the canopy contribution. Results regarding

311 contribution of forest floor to total ecosystem FAPAR were similar as those observed for albedo, i.e. there were differences

312 between tree species and decreasing trends with increasing SZA (Table 5).

313

314 The differences in albedos between coniferous species, i.e. black spruce vs. white spruce, and Scots pine vs. Norway spruce,

315 were almost nonexistent when comparing albedos obtained in black soil simulations (Table 5). This indicates that at least

316 some of the differences in albedos between coniferous species are explained by the varying forest floor contribution between

317 species. However, the differences in albedos between coniferous forests of Finland and Alaska remained, indicating that

318 other factors than forest floor influenced the species differences between the study areas.

319

320 FAPAR$_{CAN}$ varied notably more than albedo when comparing forests of same height, particularly at small SZAs (Fig. 4, Fig.

321 5). This can be explained by the link of FAPAR$_{CAN}$ with canopy interception. Interception was tightly related with LAI$_{eff}$ (not

322 shown), and it determined FAPAR$_{CAN}$ almost directly, because the foliage absorbed strongly at PAR wavelengths (Fig. 3a)

323 and therefore the multiple scattering was negligible. LAI$_{eff}$, in turn, varied considerably between forests of same height. The

324 outliers (tall trees, low FAPAR$_{CAN}$) in Fig. 5d were plots that had only few trees and therefore very low LAI$_{eff}$. Similarly,

325 Scots pine had lower FAPAR$_{CAN}$ compared to other species with same height (Fig. 5d). Further examination revealed that

326 Scots pine had short crowns and therefore low LAI$_{eff}$, although the leaf area per unit crown volume did not differ from the

327 other coniferous species. The strong link between FAPAR$_{CAN}$ and LAI$_{eff}$ explained also the observed species- and SZA

328 dependencies of FAPAR$_{CAN}$. At the lowest SZA (40°) the species-specific FAPAR$_{CAN}$ (Table 4) was strongly correlated with

329 species-specific LAI$_{eff}$ (Table 1) (r = 0.93). At large SZAs the canopy interception approached 100% at almost all LAI$_{eff}$

330 values (cf. Fig. 5c,d) and FAPAR$_{CAN}$ was therefore mainly determined by the absorption of the foliage at PAR wavelengths.

331 Leaves of broadleaved trees absorbed less than conifer needles, which explains why FAPAR$_{CAN}$ of broadleaved species did

332 not increase as rapidly as a function of SZA as did FAPAR$_{CAN}$ of coniferous species (Table 4).

333 **3.2   Relation of albedo to FAPAR**

334 FAPAR$_{CAN}$ was negatively correlated with albedo in conifer dominated forests (Fig. 8). The correlation was strongest at the

335 smallest SZA (r = -0.91, r = -0.90) and weakest at the largest SZA (r = -0.63, r = -0.59). When including mixed plots and the

336 plots dominated by broadleaved trees, correlation of FAPAR$_{CAN}$ to albedo varied from almost nonexistent in Alaska (r

337 ranging from -0.17 to 0.07) to moderate in Finland (r ranging from -0.62 to -0.30). The higher correlation in Finland can be

338 explained by the small number of broadleaved dominated forests in our data from Finland. In addition to the proportion of

339 broadleaved trees, variation in forest floor characteristics influenced the albedo-FAPAR$_{CAN}$ relations by altering the albedo

340 values (Fig. 8). The effect of forest floor was seen in relatively sparse canopies only. For example, at SZA of 40° the effect

341 of forest floor on albedo started to show at FAPAR$_{CAN}$ values below 0.5 (Fig. 8). Remembering that FAPAR$_{CAN}$ was tightly

342 related to LAI$_{eff}$, this value corresponds LAI$_{eff}$ of approx. 1. FAPAR$_{TOT}$ was strongly and negatively correlated with albedo (r

343 ranging from -0.97 to -0.88). The only plots that deviated from this otherwise strong relation were those Scots pine plots that

344 had low FAPAR$_{TOT}$ and xeric forest floor.

345 **3.3   Relative importance of density and tree species**

346 The variation in density of forests was larger in Alaska than in Finland; the 5th and 95th percentiles of basal area were 8 and

347 43 m^2 ha^{-1} in Alaska, and 10 and 34 m^2 ha^{-1} in Finland. In both study areas, decrease in basal area resulted in higher albedo

348 but lower FAPAR$_{CAN}$. At the smallest SZA (40°) the decrease in basal area from its 95th to 5th percentile resulted in increase

349 of albedo by 36% in Alaska and by 21% in Finland (Fig. 9). Correspondingly, FAPAR$_{CAN}$ decreased by 48% in Alaska and

350 by 44% in Finland. When SZA increased, the response of FAPAR$_{CAN}$ to basal area became weaker. For example, at SZA of

351 70° the basal area could be reduced to approx. 20 m^2 ha^{-1} with equal relative changes in albedo and FAPAR$_{CAN}$ (Fig. 9b). At

352 the largest SZA (80°) both albedo and FAPAR$_{CAN}$ varied very little (max. 6%) between the 5th and 95th basal area

353 percentiles. In other words, the effect of basal area depended strongly on SZA. However, the relative decrease of FAPAR$_{CAN}$

354 with decreasing basal area was always larger than or equal to the relative increase in albedo.

355

356 Increasing the proportion of broadleaved trees increased the albedos considerably more than did reduction in basal area (Fig.

357 9c,d). The effect of broadleaved trees was slightly smaller in sparse than in dense forests. For example, at SZA of 40°,

358 increasing the broadleaved proportion from 0–10% to 90–100% resulted in relative increase of albedo by 130% (in Alaska)

359 and 80% (in Finland) in forests with high basal area (i.e., basal area percentiles from 70th to 100th). In forests with low basal

360 area (i.e., basal area percentiles from 0th to 30th) the corresponding figures were 112% (Alaska) and 71% (Finland). The

361 smaller relative increase in Finland is explained by the higher albedo of Finnish coniferous forests, because the albedos of

362 broadleaved species did not differ between Alaska and Finland. FAPAR$_{CAN}$ was almost independent on the proportion of

363 broadleaved trees, except for large SZAs where FAPAR$_{CAN}$ tended to decrease slightly when broadleaved proportion

364 increased (Fig. 9d). This is explained by the fact that at large SZAs FAPAR$_{CAN}$ was mainly determined by the absorption of

365 canopy elements, and the absorption was lower for broadleaved than for coniferous trees.

366 **4   Discussion**

367 Despite recent studies published on the relationships between albedo and boreal forest structure, and despite the widespread

368 use of FAPAR to monitor vegetation productivity, the physical link between forest albedo and productivity has been poorly

369 understood. To our knowledge, the relationship between these two quantities has not been quantified earlier for an extensive

370 geographical area. Another gap in the discussion has been the role of latitude: solar paths vary across the biome, and

371 therefore, need to be taken into account before making any generalizations on how altering forest structure through

372 silvicultural operations can be used to influence albedo (and furthermore, climate).

373

374 Our results show that albedo and FAPAR$_{CAN}$ are tightly linked in boreal coniferous forests. The prerequisites for this are that

375 there is only a limited proportion of broadleaved trees present in the forest and that the tree canopy is not very sparse (i.e.

376 LAI is not very low). The explanation for the tight connection between albedo and FAPAR$_{CAN}$ is that they respond with

377 opposite trends to forest structural variables. However, the shapes of these trends depended on solar angle which was also

378 reflected in the albedo vs. FAPAR$_{CAN}$ relations. This underlines the importance of taking into account latitude and season

379 (i.e. solar angle) when evaluating climate impacts of forests even within one biome. FAPAR$_{TOT}$ was also tightly linked with

380 albedo. Because FAPAR$_{TOT}$ equals one minus PAR albedo, this finding indicates that PAR albedo and shortwave albedo of

381 vegetation are correlated. However, the overall variation in FAPAR$_{TOT}$ was small in magnitude, and therefore the total

382 ecosystem productivity is highly independent on forest structure, at least when comparing forests with similar site fertilities.

383

384 The responses of albedo to tree species and forest structure were similar across the biome in Alaska and Finland. This
385 corroborates findings in previous, local studies (Amiro et al., 2006; Bright et al., 2013; Lukeš et al., 2014; Kuusinen et al.
386 2014; Kuusinen et al., 2016). Also the results regarding overall level of FAPAR$_{CAN}$, and the dependence of FAPAR$_{CAN}$ on
387 tree species were similar to earlier studies (Roujean, 1999; Steinberg et al., 2006). However, as our study was based on
388 extensive field data from two continents, drawing more general conclusions on how forest structure, albedo and productivity
389 are interconnected is now possible. In addition, to our knowledge only one study has previously evaluated the forest floor
390 contribution to albedo (Kuusinen et al., 2015). We showed that forest floor vegetation (which is often in practical forestry
391 e.g. a proxy for site fertility type) can significantly contribute to forest albedo; its average contribution can be up to 50%,
392 varying between forests dominated by different tree species. Similarly, the average contribution of forest floor to total
393 ecosystem FAPAR can be up to or even over 50%, as reported previously also by Ikawa et al. (2015) for an eddy-covariance
394 study site in Alaska. In other words, even though forest floor vegetation often contributes only little to, for example, total
395 forest biomass, it can have a significant role as a key driving factor of forest albedo and ecosystem productivity.

396

397 The black soil simulations that we conducted in order to quantify the contribution of forest floor explained also why the
398 albedo increased as a function of solar zenith angle. From previous simulation studies it is known that when the sun
399 approaches the horizon, the path length of radiation and therefore scattering from the canopy layer increase while the
400 contribution of forest floor decreases (Kimes et al., 1987; Ni & Woodcock, 2000). The net effect is dependent on the density
401 (gap fractions) of the canopy layer, and on the reflectance of the forest floor: if the canopy is sparse or clumped, or if the
402 reflectance of the forest floor is high, it is likely that increasing the solar zenith angle reduces the forest floor contribution
403 more than it increases the scattering from canopy. Our results generalize the findings of these previous studies that examined
404 only few stands locally. It should be noted that our results apply only to summertime conditions. If the forest floor has high
405 reflectance due to e.g. snow cover, a decrease of albedo as a function of solar zenith angle is expected to be observed more
406 often (Ni & Woodcock, 2000).

407

408 We observed some interesting differences between Alaskan and Finnish datasets which deserve to be highlighted. Even
409 though our field data do not represent a probability sample they are still well representative of the forests in the study areas.
410 The mean albedo was higher in Alaska than in Finland, because of the higher proportion of broadleaved species in Alaska.
411 However, the coniferous forests in Alaska had lower albedos than those in Finland. There is some previous evidence to
412 support this, because the lowest values reported by Amiro et al. (2006) for spruce forests in Alaska are lower than those
413 reported by Kuusinen et al. (2014) for spruce in Finland. Because the difference remained also when assuming black soil, the
414 reason is in the properties of the canopy layer. Particularly, the low reflectance of bark in the Alaskan species (Fig. 3b)
415 explains part of the difference.

416

417   Radiative transfer models offer a useful tool for assessing the radiation regime of forests, especially when the modeling
418   approach can utilize readily available common forest inventory databases. Validating the simulated albedo and FAPAR
419   values, however, is challenging. Even though international model intercomparison efforts such as RAMI (Widlowski et al.,
420   2007) provide a rigorous set of reports on performance of radiative transfer models, the quality of available input data in
421   each study where a radiative transfer model is applied is crucial. For example, the forest floor albedos that we calculated
422   from the available reflectance spectra (Fig. 3) were clearly higher (0.18−0.23) than forest floor albedos measured in the field
423   at other boreal sites (approx. 0.15 in Manninen & Riihelä, 2008; Manninen & Riihelä, 2009; Kuusinen et al., 2014). If we
424   had scaled our reflectance factors in order to obtain forest floor albedos of 0.15, the simulated forest albedos would have
425   decreased by 7–10%. Furthermore, including also the UV region in the simulations would have reduced the simulated
426   albedos by up to 7%, assuming that the optical properties of the canopy and forest floor are similar at UV than at 400 nm.
427   However, particularly the lack of field measured spectra for some of the Alaskan species is a limitation of our study and
428   shows that there is an urgent need for comprehensive spectral database of boreal tree species.

429

430   Our results regarding basal area give an idea of the magnitude of the effects that varying thinning regimes could have on
431   forest albedo and productivity. The effect of thinnings on albedo have previously been estimated mainly by in situ
432   measurements at few selected sites (Kirschbaum et al., 2011; Kuusinen et al., 2014). In our study, reduction in the basal area
433   reduced $FAPAR_{CAN}$ equally or more compared to how albedo changed. In contrast to basal area, the proportion of
434   broadleaved trees had a notably larger effect on forest albedo while having only a negligible influence on forest productivity
435   ($FAPAR_{CAN}$). The relative importance of basal area and tree species nevertheless depends on the spectral properties of the
436   tree species and forest floor. Based on our results, the effect of thinning (removal of basal area) on albedo and FAPAR
437   depends on solar angle. Therefore, the influence of thinning on forest productivity differs between latitudes. Furthermore,
438   because the basal area influenced albedo and $FAPAR_{CAN}$ less at large sun zenith angles, the effects of thinning integrated
439   over entire rotation period may not be as large as they seem when studying them only at solar noon.

440

441   Global satellite products have provided us insight on coarse-scale trends of albedo in different biomes. However, their
442   weakness is that even though we can establish correlations between changes in albedo and changes in land cover, we are still
443   not able to identify and quantify the biophysical factors which cause the albedo of a forest area to change. In addition, a
444   specific challenge in coupling forest management operations with changes in satellite-based albedo products is that the scale
445   of these operations significantly differs in North America and Northern Europe, and often does not directly correspond to the
446   spatial resolution of current albedo products. With an understanding of the consequences of, for example, forest management
447   practices on the albedo, best-practice recommendations for forest management in future climate mitigation policies will
448   become more justified. By coupling extensive field inventory data sets and radiative transfer modeling, we showed that
449   albedo and $FAPAR_{CAN}$ are tightly linked in boreal coniferous forests at stand level. However, the relation is weaker if the
450   forest has deciduous admixture, or if the canopies are sparse and at the same time the species composition (i.e. optical

properties) of the forest floor vary. Because the shape of the relationship between albedo and FAPAR$_{CAN}$ was shown to depend on solar angle, studies evaluating the climate effects of forest management strategies need to consider latitudinal effects due to varying solar paths. The comparisons between Alaska and Finland revealed that albedo and FAPAR$_{CAN}$ differ between geographical regions because of the differences in forest structure. However, regardless of geographical region in the boreal zone, the potential of using thinning to increase forest albedo may be limited compared to the effect of favoring broadleaved species.

Data availability

Data from Co-operative Alaska Forest Inventory prior to 2009 are available at LTER Network Data Portal (http://dx.doi.org/10.6073/pasta/d442e829a1adf7da169b6076826de563). Forest inventory data from Finland are described in Korhonen (2011) and Majasalmi et al. (2015). Leaf and needle optical properties measured in Hyytiälä are reposited at SPECCHIO database (http://www.specchio.ch/), and those measured in Superior National Forest are reposited at ORNL DAAC by NASA (http://dx.doi.org/10.3334/ORNLDAAC/183). Forest floor spectra were presented in Fig. 3 of this manuscript.

Acknowledgments

This study was funded in parts by the Academy of Finland projects BOREALITY and SATLASER, and by the Davis College of Agriculture, Natural Resources & Design, West Virginia University, under the US Department of Agriculture (USDA) McIntire–Stennis Funds WVA00106. We thank Petr Lukeš and Matti Mõttus for advice on radiative transfer modeling, and Titta Majasalmi, Pekka Voipio, Jussi Peuhkurinen and Maria Villikka for organizing the measurements of field plots in Finland. We also thank the School of Natural Resources and Agricultural Sciences, University of Alaska for the establishment and maintenance of the Co-operative Alaska Forest Inventory. The forest floor reflectances at Poker Flag Research Range were obtained under the JAMSTEC and IARC/UAF collaborative study (PI: Rikie Suzuki).

References

Alkama, R. and Cescatti, A.: Biophysical climate impacts of recent changes in global forest cover, Science, 351, 600–604, 2016.

Amiro, B. D., Orchansky, A. L., Barr, A. G., Black, T. A., Chambers, S. D., Chapin, F. S., Goulden, M. L., Litvak, M., Liu, H. P., McCaughey, J. H., McMillan, A. and Randerson, J. T.: The effect of post-fire stand age on the boreal forest energy balance, Agric. For. Meteorol., 140, 41–50, 2006.

478 Bond-Lamberty, B., Wang, C., Gower, S. T. and Norman, J.: Leaf area dynamics of a boreal black spruce fire

479 chronosequence., Tree Physiol., 22, 993–1001, 2002.

480 Bragg, D. C.: A local basal area adjustment for crown width prediction, North. J. Appl. For., 18, 22–28, 2001.

481 Bright, R. M., Antón-Fernández, C., Astrup, R., Cherubini, F., Kvalevåg, M. and Strømman, A. H.: Climate change

482 implications of shifting forest management strategy in a boreal forest ecosystem of Norway, Glob. Chang. Biol., 20, 607–

483 621, 2014.

484 Bright, R. M., Astrup, R. and Strømman, A. H.: Empirical models of monthly and annual albedo in managed boreal forests

485 of interior Norway, Clim. Change, 120, 183–196, 2013.

486 Cajander, A. K.: Forest types and their significance. Acta Forestalia Fennica, 56, 1–71, 1949.

487 Chasmer, L., Hopkinson, C., Treitz, P., McCaughey, H., Barr, A. and Black, A.: A lidar-based hierarchical approach for

488 assessing MODIS fPAR, Remote Sens. Environ., 112, 4344–4357, 2008.

489 Gobron, N., Verstraete, M.M.: Assessment of the status of the development of the standards for the terrestrial essential

490 climate variables. T10 Fraction of Absorbed Photosynthetically Active Radiation (FAPAR). V8, GTOS65, pp. 1–24. NRC,

491 FAO, Rome, Italy, 2009.

492 Hall, F. G., Huemmrich, K. F., Strebel, D. E., Goetz, S. J., Nickeson, J. E., and Woods, K. D.: SNF Leaf Optical Properties:

493 Cary-14. [Superior National Forest Leaf Optical Properties: Cary-14]. Data set. Available on-line [http://www.daac.ornl.gov]

494 from Oak Ridge National Laboratory Distributed Active Archive Center, Oak Ridge, Tennessee, U.S.A, 1996. Based on

495 Hall, F. G., Huemmrich, K. F., Strebel, D. E., Goetz, S. J., Nickeson, J. E., and Woods, K. D.: Biophysical, Morphological,

496 Canopy Optical Property, and Productivity Data from the Superior National Forest, NASA Technical Memorandum 104568,

497 National Aeronautics and Space Administration, Goddard Space Flight Center, Greenbelt, Maryland, U.S.A., 1992.

498 doi:10.3334/ORNLDAAC/183

499 Hotanen, J-P., Nousiainen, H., Mäkipää, R., Reinikainen, A., Tonteri, T.: Metsätyypit – opas kasvupaikkojen luokitteluun (In

500 Finnish), pp. 1–192. Metsäkustannus Oy, Porvoo, Finland, 2013.

501 Ikawa, H., Nakai, T., Busey, R. C., Kim, Y., Kobayashi, H., Nagai, S., Ueyama, M., Saito, K., Nagano, H., Suzuki, R. and

502 Hinzman, L.: Understory CO_2, sensible heat, and latent heat fluxes in a black spruce forest in interior Alaska, Agric. For.

503 Meteorol., 214-215, 80–90, 2015.

504 Jakobsons, A.: Sambandet mellan trädkronans diameter och andra trädfaktorer, främst brösthöjdsdiametern: analyser

505 grundade på riksskogstaxeringens provträdsmaterial (the relationship between crown diameter and other tree factors,

506 diameter at breast height in particular: analysis based on the sample tree material of the National Forest Inventory).

507 Stockholms skoghögsskolan, institutionen för skogstaxering (Rapporter och uppsatser 14), pp.1–75, 1970.

508 Kimes, D. S., Sellers, P. J. and Newcomb, W. W.: Hemispherical reflectance variations of vegetation canopies and

509 implications for global and regional energy budget studies, J. Clim. Appl. Meteorol., 26, 959–972, 1987.

510 Kirschbaum, M. U. F., Whitehead, D., Dean, S. M., Beets, P. N., Shepherd, J. D. and Ausseil, A. G. E.: Implications of

511 albedo changes following afforestation on the benefits of forests as carbon sinks, Biogeosciences, 8, 3687–3696, 2011.

512 Korhonen, L.: Estimation of boreal forest canopy cover with ground measurements, statistical models and remote sensing.

513 Dissertationes Forestales, 115, 1–56, 2011.

514 Kull, O. and Niinemets, U.: Variations in Leaf Morphometry and Nitrogen Concentration in Betula-Pendula Roth, Corylus-

515 Avellana L and Lonicera-Xylosteum L, Tree Physiol., 12, 311–318, 1993.

516 Kuusinen, N., Kolari, P., Levula, J., Porcar-Castell, A., Stenberg, P. and Berninger, F.: Seasonal variation in boreal pine

517 forest albedo and effects of canopy snow on forest reflectance, Agric. For. Meteorol., 164, 53–60, 2012.

518 Kuusinen, N., Tomppo, E. and Berninger, F.: Linear unmixing of MODIS albedo composites to infer subpixel land cover

519 type albedos, Int. J. Appl. Earth Obs. Geoinf., 23, 324–333, 2013.

520 Kuusinen, N., Lukeš, P., Stenberg, P., Levula, J., Nikinmaa, E. and Berninger, F.: Measured and modelled albedos in Finnish

521 boreal forest stands of different species, structure and understory, Ecol. Modell., 284, 10–18, 2014.

522 Kuusinen, N., Stenberg, P., Tomppo, E., Bernier, P., Berninger, F., Kuusinen, N., Stenberg, P., Berninger, F., Tomppo, E.

523 and Bernier, P.: Variation in understory and canopy reflectance during stand development in Finnish coniferous forests, Can.

524 J. For. Res, 45, 1077–1085, 2015.

525 Kuusinen, N., Stenberg, P., Korhonen, L., Rautiainen, M. and Tomppo, E.: Structural factors driving boreal forest albedo in

526 Finland, Remote Sens. Environ., 175, 43–51, 2016.

527 Kuusk, A. and Nilson, T.: A directional multispectral forest reflectance model, Remote Sens. Environ., 72, 244–252, 2000.

528 Lang, M., Kuusk, A., Nilson, T., Lükk, T., Pehk, M., Alm, G.: Reflectance spectra of ground vegetation in sub-boreal

529 forests. Web page. Available online. http://www.aai.ee/bgf/ger2600/ (from Tartu Observatory, Estonia. Accessed 6 Feb,

530 2013), 2002.

531 Liang, J., Zhou, M., Tobin, P. C., McGuire, A. D. and Reich, P. B.: Biodiversity influences plant productivity through niche-

532 efficiency., Proc. Natl. Acad. Sci. U. S. A., 112, 5738-5743, 2015.

533 Lukeš, P., Stenberg, P. and Rautiainen, M.: Relationship between forest density and albedo in the boreal zone, Ecol. Modell.,

534 261-262, 74–79, 2013a.

535 Lukeš, P., Stenberg, P., Rautiainen, M., Mõttus, M. and Vanhatalo, K. M.: Optical properties of leaves and needles for boreal

536 tree species in Europe, Remote Sens. Lett., 4, 667–676, 2013b.

537 Lukeš, P., Rautiainen, M., Manninen, T., Stenberg, P. and Mõttus, M.: Geographical gradients in boreal forest albedo and
538 structure in Finland, Remote Sens. Environ., 152, 526–535, 2014.

539 Majasalmi, T., Rautiainen, M. and Stenberg, P.: Modeled and measured fPAR in a boreal forest: Validation and application
540 of a new model, Agric. For. Meteorol., 189-190, 118–124, 2014.

541 Majasalmi, T., Rautiainen, M., Stenberg, P. and Manninen, T.: Validation of MODIS and GEOV1 fPAR Products in a
542 Boreal Forest Site in Finland, Remote Sens., 7, 1359–1379, 2015.

543 Malone, T., Liang, J., Packee, E.C.: Cooperative Alaska Forest Inventory. General Technical Report PNW-GTR-785, USDA
544 Forest Service, Pacific Northwest Research Station, 32 Portland, OR, pp. 1–58, 2009.

545 Manninen, T., Riihelä, A.: Subarctic boreal forest albedo estimation using ENVISAT ASAR for BRDF determination.
546 Proceedings of IGARSS'08, July 6 11, 2008, CD, p. 1–4, 2008.

547 Manninen, T., Riihelä, A.: ENVISAT/ASAR VV/HH backscattering and the radiation characteristics of Subarctic boreal
548 forest. Proceedings of PolInSAR 2009, 26–30 January 2009, Frascati, Italy, Special publication of ESA SP-668, pp. 1–8,
549 2009.

550 Mõttus, M., Stenberg, P. and Rautiainen, M.: Photon recollision probability in heterogeneous forest canopies: Compatibility
551 with a hybrid GO model, J. Geophys. Res. Atmos., 112, 1–10, 2007.

552 Naudts, K., Chen, Y., McGrath, M. J., Ryder, J., Valade, A., Otto, J., Luyssaert, S.: Europe's forest management did not
553 mitigate climate warming. Science, 351, 597–601, 2016.

554 Ni, W. and Woodcock, C. E.: Effect of canopy structure and the presence of snow on the albedo of boreal conifer forests, J.
555 Geophys. Res., 105, 11879, 2000.

556 Nilson, T.: Inversion of gap frequency data in forest stands, Agric. For. Meteorol., 98-9, 437–448, 1999.

557 Palmroth, S. and Hari, P.: Evaluation of the importance of acclimation of needle structure, photosynthesis, and respiration to
558 available photosynthetically active radiation in a Scots pine canopy, Can. J. For. Res., 31, 1235–1243, 2001.

559 Pan, Y., Birdsey, R. A., Fang, J., Houghton, R., Kauppi, P. E., Kurz, W. A., Phillips, O. L., Shvidenko, A., Lewis, S. L.,
560 Canadell, J. G., Ciais, P., Jackson, R. B., Pacala, S. W., McGuire, A. D., Piao, S., Rautiainen, A., Sitch, S. and Hayes, D.: A
561 Large and Persistent Carbon Sink in the World's Forests, Science, 333, 988–993, 2011.

562 Rautiainen, M., Suomalainen, J., Mõttus, M., Stenberg, P., Voipio, P., Peltoniemi, J. and Manninen, T.: Coupling forest
563 canopy and understory reflectance in the Arctic latitudes of Finland, Remote Sens. Environ., 110, 332–343, 2007.

564 Rautiainen, M., Mottus, M., Stenberg, P. and Ervasti, S.: Crown envelope shape measurements and models, Silva Fenn., 42,
565 19–33, 2008.

566 Rautiainen, M., Mõttus, M., Heiskanen, J., Akujärvi, A., Majasalmi, T. and Stenberg, P.: Seasonal reflectance dynamics of
567 common understory types in a northern European boreal forest, Remote Sens. Environ., 115, 3020–3028, 2011.

568 Rautiainen, M., Mõttus, M., Yáñez-Rausell, L., Homolová, L., Malenovský, Z. and Schaepman, M. E.: A note on upscaling
569 coniferous needle spectra to shoot spectral albedo, Remote Sens. Environ., 117, 469–474, 2012.

570 Reich, P. B., Ellsworth, D. S., Walters, M. B., Vose, J. M., Gresham, C., Volin, J. C. and Bowman, W. D.: Generality of leaf
571 trait relationships: A test across six biomes, Ecology, 80, 1955–1969, 1999.

572 Repola, J.: Biomass equations for birch in Finland, Silva Fenn., 42, 605–624, 2008.

573 Repola, J.: Biomass equations for Scots pine and Norway spruce in Finland, Silva Fenn., 43, 625–647, 2009.

574 Richardson, A. D., Berlyn, G. P. and Duigan, S. P.: Reflectance of Alaskan black spruce and white spruce foliage in relation
575 to elevation and latitude, Tree Physiol., 23, 537–544, 2003.

576 Roujean, J. L.: Measurements of PAR transmittance within boreal forest stands during BOREAS, Agric. For. Meteorol., 93,
577 1–6, 1999.

578 Schaaf, C. B.: Assessment of the status of the development of the standards for the terrestrial essential climate variables. T8
579 albedo and reflectance anisotropy. V12, GTOS63, pp. 1–20 NRC, FAO, Rome, 2009.

580 Serbin, S. P., Ahl, D. E. and Gower, S. T.: Spatial and temporal validation of the MODIS LAI and FPAR products across a
581 boreal forest wildfire chronosequence, Remote Sens. Environ., 133, 71–84, 2013.

582 Sigurdsson, B. D., Thorgeirsson, H. and Linder, S.: Growth and dry-matter partitioning of young Populus trichocarpa in
583 response to carbon dioxide concentration and mineral nutrient availability., Tree Physiol., 21, 941–50, 2001.

584 Smolander, H., Stenberg, P. and Linder, S.: Dependence of light interception efficiency on structural parameters, Tree
585 Physiol., 14, 971–980, 1994.

586 Steinberg, D., Goetz, S. and Hyer, E.: Validation of MODIS FPAR products in boreal forests of Alaska, IEEE Trans. Geosci.
587 Remote Sens., 44, 1818–1828, 2006.

588 Stenberg, P., Kangas, T., Smolander, H. and Linder, S.: Shoot structure, canopy openness, and light interception in Norway
589 spruce, Plant, Cell Environ., 22, 1133–1142, 1999.

590 Stenberg, P., Linder, S. and Smolander, H.: Variation in the ratio of shoot silhouette area to needle area in fertilized and
591 unfertilized Norway spruce trees., Tree Physiol., 15, 705–12, 1995.

592 Thérézien, M., Palmroth, S., Brady, R. and Oren, R.: Estimation of light interception properties of conifer shoots by an
593 improved photographic method and a 3D model of shoot structure., Tree Physiol., 27, 1375–87, 2007.

594 Thuillier, G., Hers, M., Simon, P. C., Labs, D., Mandel, H. and Gillotay, D.: Observation of the solar spectral irradiance

595 from 200 nm to 870 nm during the ATLAS 1 and ATLAS 2 missions by the SOLSPEC spectrometer, Metrologia, 35, 689–

596 695, 2003.

597 Widlowski, J. L., Taberner, M., Pinty, B., Bruniquel-Pinel, V., Disney, M., Fernandes, R., Gastellu-Etchegorry, J. P.,

598 Gobron, N., Kuusk, A., Lavergne, T., Leblanc, S., Lewis, P. E., Martin, E., Mõttus, M., North, P. R. J., Qin, W., Robustelli,

599 M., Rochdi, N., Ruiloba, R., Soler, C., Thompson, R., Verhoef, W., Verstraete, M. M. and Xie, D.: Third Radiation Transfer

600 Model Intercomparison (RAMI) exercise: Documenting progress in canopy reflectance models, J. Geophys. Res. Atmos.,

601 112, 1–28, 2007.

602 Yang, W., Kobayashi, H., Suzuki, R. and Nasahara, K.: A Simple Method for Retrieving Understory NDVI in Sparse

603 Needleleaf Forests in Alaska Using MODIS BRDF Data, Remote Sens., 6, 11936–11955, 2014.

604 Yarie, B. J., Kane, E., Hall, B.: Aboveground Biomass Equations for the Trees of Interior Alaska. AFES Bulletin, 115, 1–16,

605 2007.

Table 1. Mean (standard deviation) of forest variables by dominant tree species in Alaska and Finland. The species dominance was determined by basal area proportion: If the basal area of one of the species exceeded 80% of the total basal area, the plot was considered to be dominated by that species. The remaining plots were labeled as mixed.

Tree species	Number of plots	Stems per hectare	Diameter at breast height (cm) [1]	Height (m)	Crown ratio (%) [2]	Basal area (m^2 ha^{-1})	Effective LAI (m^2 m^{-2}) [3]
Alaska							
Black spruce	70	2361 (1542)	9.3 (3.8)	7.3 (3.2)	69 (11)	14.6 (9.3)	1.0 (0.6)
White spruce	124	806 (653)	21.3 (7.9)	14.7 (5.2)	74 (9)	22.8 (13.1)	2.4 (1.3)
Quaking aspen	22	1572 (916)	15.8 (5.1)	13.9 (3.5)	37 (7)	26.0 (8.8)	2.8 (0.9)
Black cottonwood/ balsam poplar	8	672 (658)	35.1 (14.7)	20.5 (5.8)	62 (11)	34.8 (14.5)	2.7 (1.1)
Birches	84	873 (662)	22.6 (8.4)	17.5 (2.9)	58 (11)	25.1 (8.1)	3.2 (1.4)
Mixed	276	1082 (1131)	22.0 (8.3)	15.1 (3.9)	62 (12)	25.2 (10.1)	2.7 (1.2)
All	584	1160 (1139)	20.3 (9.0)	14.4 (4.9)	64 (13)	23.6 (11.0)	2.5 (1.3)
Finland							
Scots pine	184	1165 (1301)	18.0 (8.5)	14.7 (6.4)	51 (16)	15.9 (7.7)	1.1 (0.5)
Norway spruce	115	980 (1014)	19.7 (8.9)	16.6 (6.9)	68 (15)	19.8 (9.4)	2.4 (1.1)
Broadleaved	23	1409 (1419)	13.6 (7.1)	13.9 (6.0)	62 (16)	12.6 (7.1)	1.9 (1.2)
Mixed	180	1094 (1782)	20.5 (8.0)	17.2 (5.8)	58 (14)	20.3 (9.1)	2.2 (1.1)
All	502	1109 (1444)	19.1 (8.5)	16.0 (6.4)	58 (16)	18.2 (8.9)	1.8 (1.1)

1) Definition of breast height differed between Alaska (1.37 m) and Finland (1.3 m).

2) Ratio of the length of living crown to tree height.

3) Not measured in the field. The values are calculated by the FRT model.

Table 2. Number of study plots by dominant tree species and by forest floor type. The species dominance was determined by basal area proportion: If the basal area of one of the species exceeded 80% of the total basal area, the plot was considered to be dominated by that species.

Tree species	Forest floor		
	Grass	Shrub/moss	Lichen
Black spruce	8	60	2
White spruce	13	111	0
Quaking aspen	4	18	0
Black cottonwood/balsam poplar	2	6	0
Birches	23	61	0
Mixed	40	236	0
All	90	492	2
	Herb-rich	Mesic	Xeric
Scots pine	2	145	37
Norway spruce	28	86	1
Broadleaved	8	14	1
Mixed	26	152	2
All	64	397	41

616 Table 3. Structural input parameters used in the FRT model simulations.

	Leaf mass per area (g m^{-2}) [1]	Shoot shading coefficient [2]	Shoot length (m) [3]	Branch area to leaf area ratio [4]
Alaska				
Black spruce	187	0.50	0.05	0.18
White spruce	182	0.50	0.05	0.18
Quaking aspen	57	1	0.40	0.15
Balsam poplar	86	1	0.40	0.15
Birches	54	1	0.40	0.15
Finland				
Scots pine	158	0.59	0.10	0.18
Norway spruce	200	0.64	0.05	0.18
Broadleaved	57	1	0.40	0.15

617 1) Black spruce and white spruce (Reich et al., 1999), quaking aspen and birches in Alaska (Bond-Lamberty et al., 2002),

618 balsam poplar (Sigurdsson et al., 2001), Scots pine (Palmroth & Hari, 2001), Norway spruce (Stenberg et al., 1999),

619 broadleaved species in Finland (values of birch from Kull & Niinemets, 1993)

620 2) Projected to total needle area in a shoot. Measures the effective leaf area, taking into account the self-shading of needles in

621 a shoot. Black spruce and white spruce (Thérézien et al., 2007), Scots pine (Smolander et al., 1994), Norway spruce

622 (Stenberg et al., 1995)

623 3, 4) Same values as used by Lukeš et al. (2013a)

624 Table 4. Albedo, FAPAR$_{CAN}$, and FAPAR$_{TOT}$ by dominant tree species and SZA. The reported value for given species is the

625 mean of plots in which the basal area proportion of that species exceeded 80%. The number of plots and mean forest

626 variables for each species are reported in Table 1.

Tree species	SZA				
	40°	50°	60°	70°	80°
Albedo					
Black spruce	0.121	0.122	0.124	0.128	0.137
White spruce	0.091	0.094	0.097	0.103	0.114
Broadleaved (Alaska)	0.194	0.204	0.218	0.236	0.262
Scots pine	0.144	0.147	0.152	0.159	0.172
Norway spruce	0.110	0.114	0.120	0.128	0.141
Broadleaved (Finland)	0.207	0.218	0.231	0.248	0.273
FAPAR$_{CAN}$					
Black spruce	0.47	0.53	0.61	0.72	0.86
White spruce	0.72	0.77	0.84	0.90	0.95
Broadleaved (Alaska)	0.78	0.82	0.86	0.89	0.91
Scots pine	0.50	0.57	0.65	0.75	0.86
Norway spruce	0.73	0.79	0.84	0.89	0.92
Broadleaved (Finland)	0.60	0.65	0.71	0.76	0.81
FAPAR$_{TOT}$					
Black spruce	0.97	0.97	0.97	0.97	0.97
White spruce	0.98	0.98	0.98	0.98	0.98
Broadleaved (Alaska)	0.95	0.95	0.94	0.94	0.93
Scots pine	0.97	0.97	0.97	0.97	0.96
Norway spruce	0.97	0.97	0.97	0.97	0.97
Broadleaved (Finland)	0.95	0.95	0.94	0.94	0.93

627

Table 5. Canopy and forest floor contributions to albedo, and forest floor contribution to $FAPAR_{TOT}$ by dominant tree species and SZA. The reported value for given species is the mean of plots in which the basal area proportion of that species exceeded 80%. Note that the values are directly comparable to the species specific forest albedos and FAPAR values reported in Table 4, i.e. exactly the same plots were used to calculate the average values in both tables.

Tree species	SZA				
	40°	50°	60°	70°	80°
Forest albedo when assuming black soil					
Black spruce	0.053	0.059	0.069	0.084	0.108
White spruce	0.062	0.068	0.076	0.087	0.104
Broadleaved (Alaska)	0.169	0.182	0.199	0.221	0.251
Scots pine	0.075	0.084	0.096	0.114	0.140
Norway spruce	0.079	0.087	0.097	0.109	0.128
Broadleaved (Finland)	0.140	0.155	0.173	0.197	0.231
Contribution of forest floor to total forest albedo, %					
Black spruce	52.9	48.0	41.4	32.4	20.2
White spruce	27.9	23.7	19.0	13.7	8.0
Broadleaved (Alaska)	12.9	10.9	8.7	6.5	4.3
Scots pine	45.6	40.6	34.5	26.8	17.9
Norway spruce	23.5	19.7	15.8	11.9	8.0
Broadleaved (Finland)	32.7	29.5	25.9	21.9	17.1
Contribution of forest floor to $FAPAR_{TOT}$, %					
Black spruce	50.1	44.1	36.0	25.1	11.1
White spruce	26.4	20.6	14.5	8.3	2.6
Broadleaved (Alaska)	16.9	12.5	8.3	4.6	2.0
Scots pine	46.3	39.8	31.7	21.5	10.5
Norway spruce	24.4	18.7	13.2	8.3	4.4
Broadleaved (Finland)	34.7	29.3	23.5	17.7	12.4

632
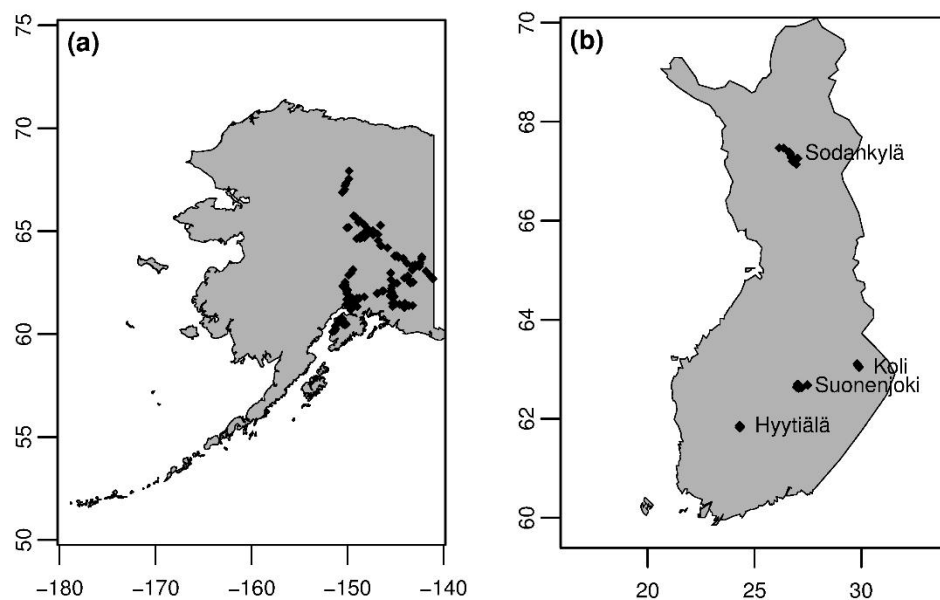
633

634   Figure 1. Location of the field plots.
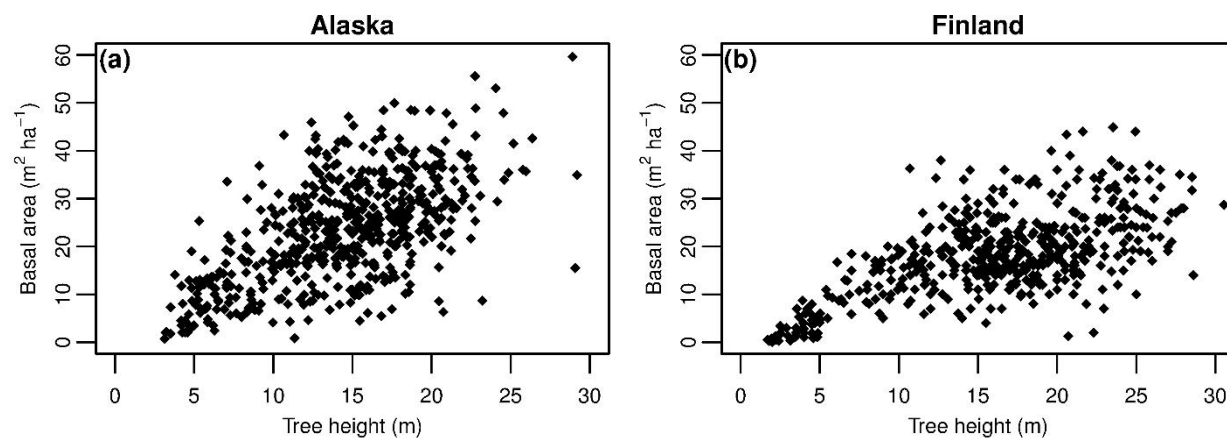
635

636 Figure 2. Basal area against tree height in the study plots in Alaska (a) and Finland (b).
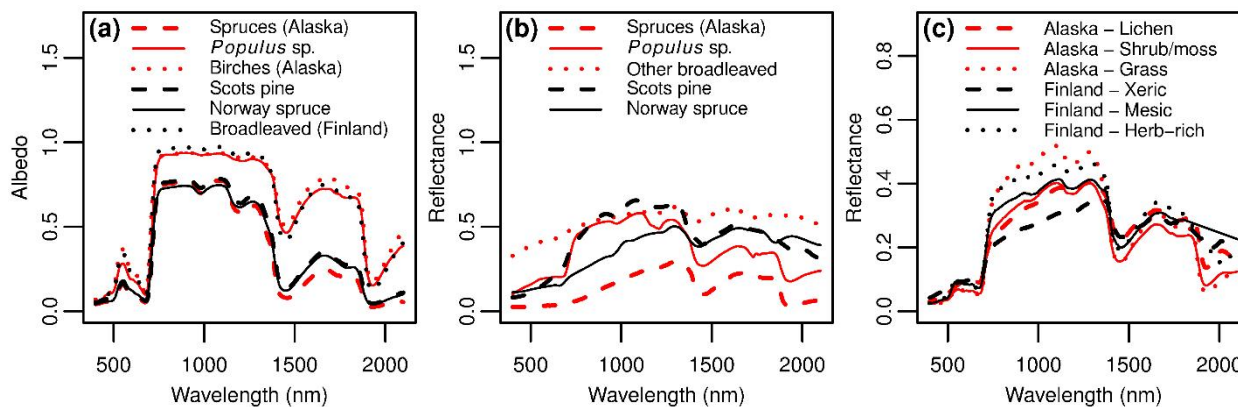
Figure 3. Spectra of vegetation elements used in the simulations: (a) leaves/shoots, (b) bark, (c) forest floor. The values for leaf and shoot are single scattering albedos (reflectance + transmittance), and the values for bark and forest floor are reflectance factors.

641
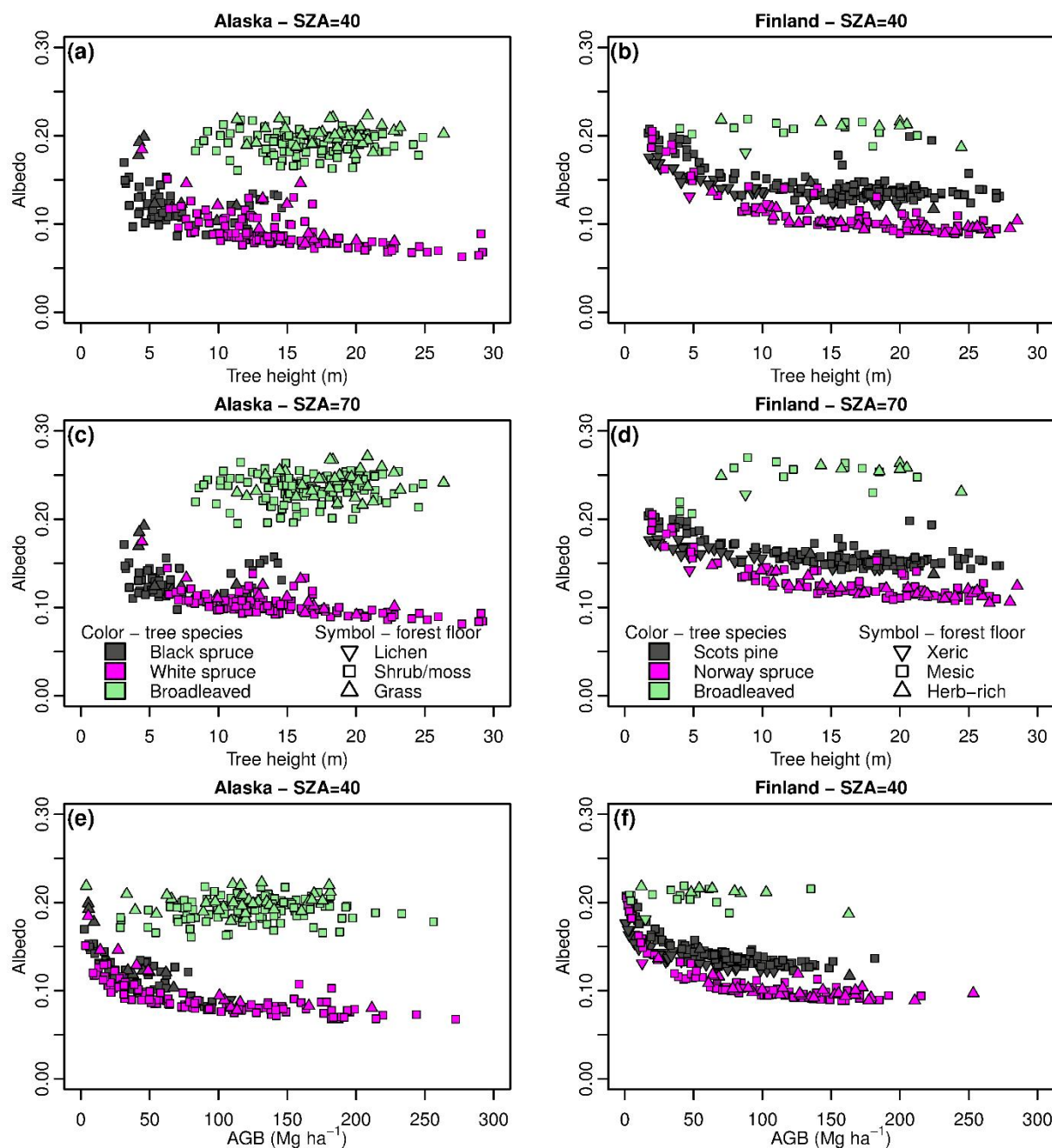
Figure 4. Forest albedo as a function of tree height (a–d) and AGB (e–f). Relations to tree height are shown for two SZAs, 40° (a–b) and 70° (c–d), representing solar noon at midsummer and the annual average in the study regions. Left hand column shows the results for the Alaskan data, and right hand column for the Finnish data. The figures show only monospecific plots, i.e. plots in which the basal area proportion of one of the species exceeded 80%.

646
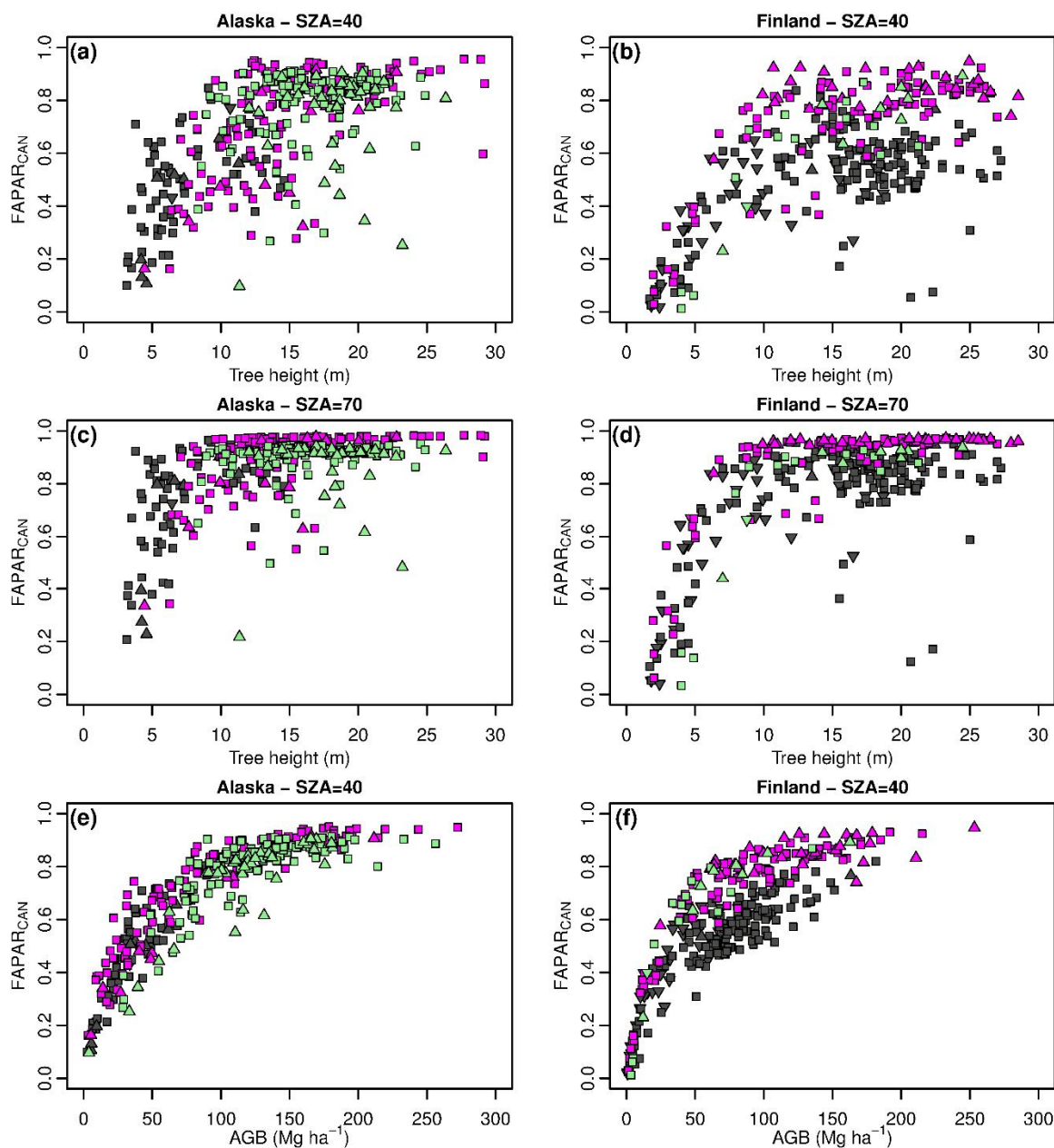
Figure 5. FAPAR$_{CAN}$ as a function of tree height (a–d) and AGB (e–f). Relations to tree height are shown for two SZAs, 40°
(a–b) and 70° (c–d), representing solar noon at midsummer and the annual average in the study regions. Left hand column
shows the results for the Alaskan data, and right hand column for the Finnish data. The figures show only monospecific plots
i.e. plots in which the basal area proportion of one of the species exceeded 80%. For explanation of the symbols, see legend
in Fig. 4.
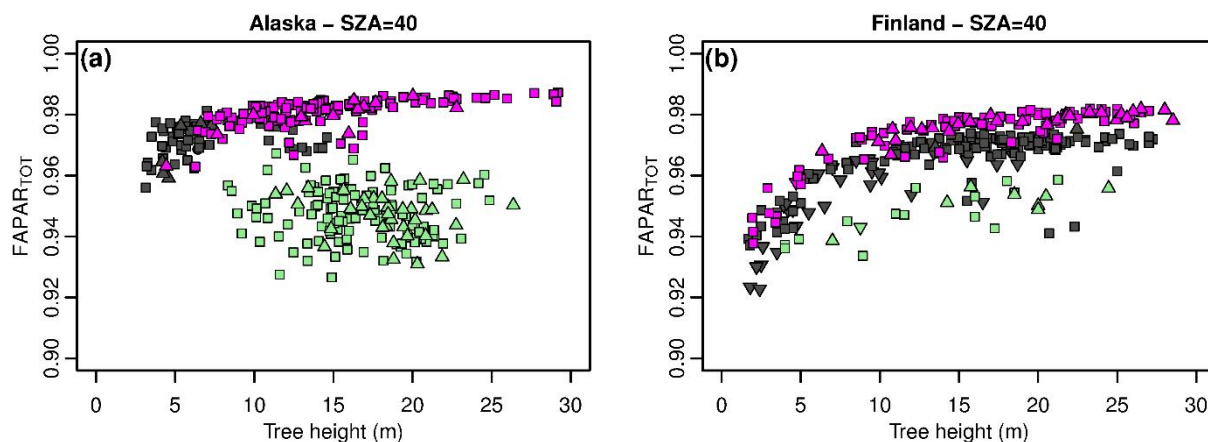
652

653 Figure 6. FAPAR$_{TOT}$ as a function of tree height at SZA of 40°. The figures show only monospecific plots i.e. plots in which

654 the basal area proportion of one of the species exceeded 80%. For explanation of the symbols, see legend in Fig. 4.
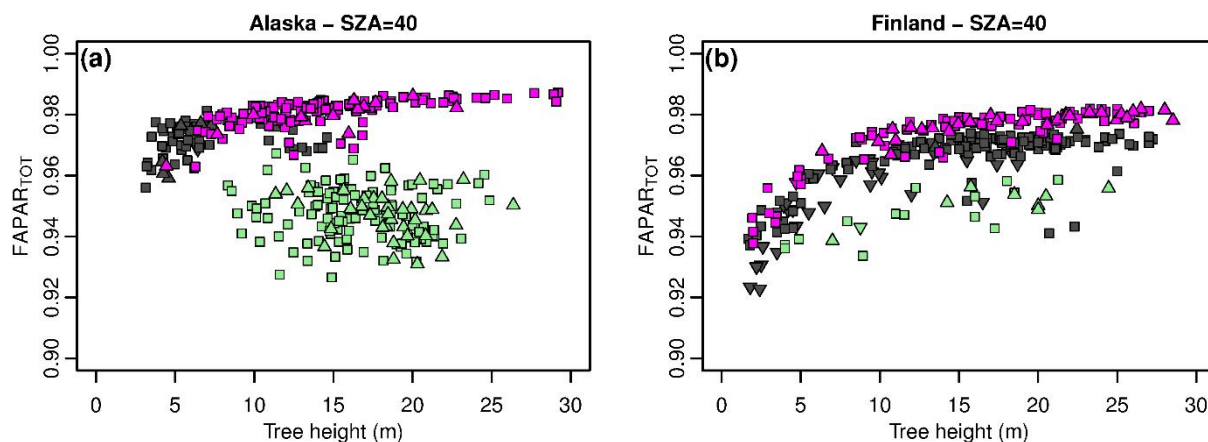
Figure 7. Canopy and forest floor contributions to forest albedo as function of tree height. Canopy contribution was obtained by assuming black soil in the simulation. Forest floor contribution was obtained by subtracting the canopy contribution from the total forest albedo. The data shown are from Norway spruce dominated forests in Finland.
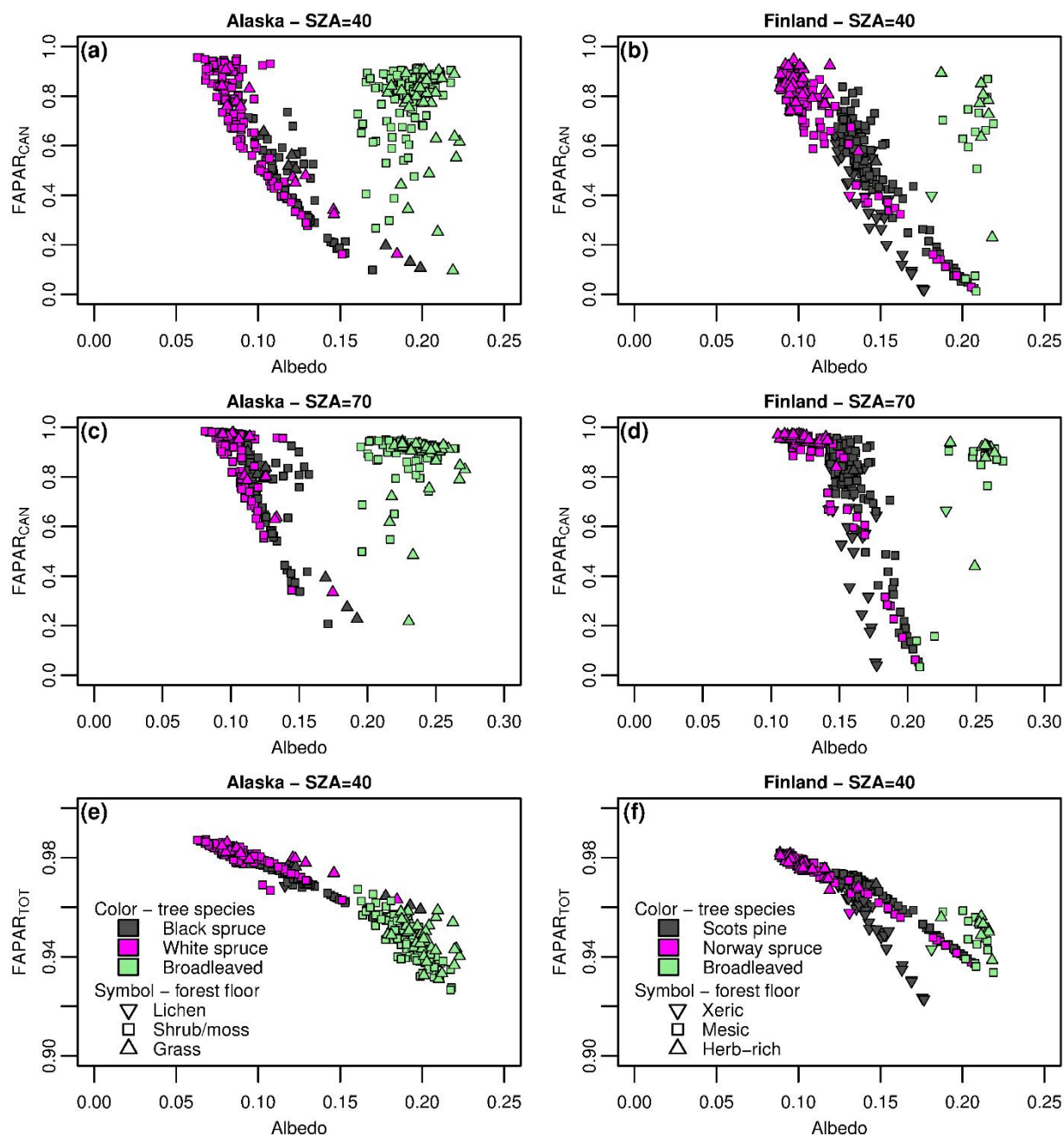
660 Figure 8. Relation of FAPAR to forest albedo by dominant tree species. The figures show only plots that were dominated by

661 one species i.e. in which the basal area proportion of one of the species exceeded 80%. a–d: $FAPAR_{CAN}$ against albedo at

662 two SZAs, 40° and 70°, representing solar noon at midsummer and the annual average in the study regions; e–f: $FAPAR_{TOT}$

663 against albedo at SZA of 40°.
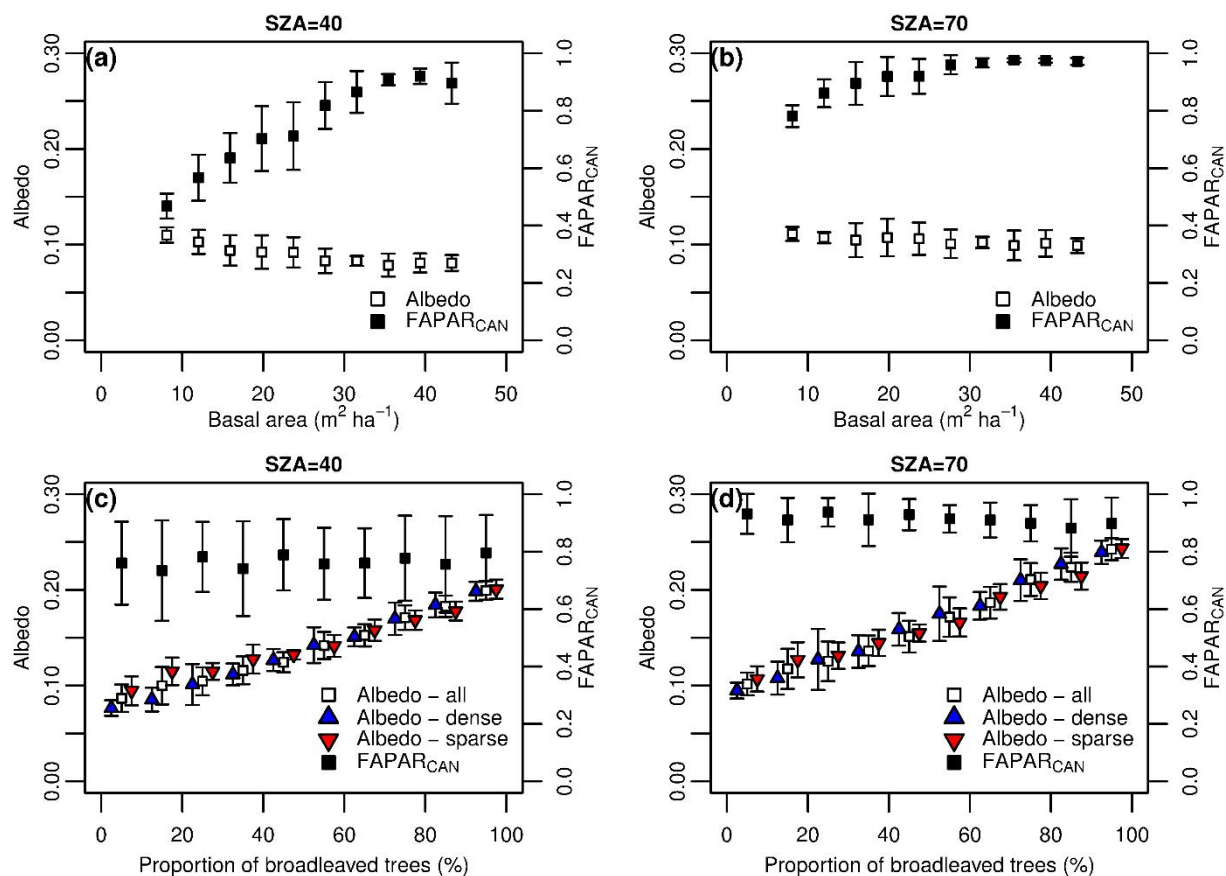
Figure 9. Effect of basal area (a–b) and proportion of broadleaved trees (c–d) on albedo and FAPAR$_{CAN}$ at sun zenith angles of 40° and 70° in Alaska. Points represent mean and whiskers the standard deviation in ten equally spaced classes. Effect of broadleaved proportion on albedo is presented separately for dense (basal area > 31 m^2 ha^{-1}) and sparse (basal area < 21 m^2 ha^{-1}) forest. These limits correspond to 30th and 70th percentiles of basal area in Alaskan data. The points representing dense and sparse forest are shifted along the x axis in order to make them visible.